Chemistry & Biology, Vol. 10, 733–742, August, 2003, ©2003 Elsevier Science Ltd. All rights reserved. DOI 10.1016/S1074-5521(03)00170-4

Cell-Active Dual Specificity Phosphatase Inhibitors Identified by High-Content Screening

Andreas Vogt,[1] Kathleen A. Cooley,[1] Marni Brisson,[1] Michael G. Tarpley,[1] Peter Wipf,[2] and John S. Lazo[1,*]
[1]Department of Pharmacology
[2]Department of Chemistry
University of Pittsburgh
Pittsburgh, Pennsylvania 15261

Summary

Phosphorylation of extracellular signal-regulated kinase (Erk) is tightly controlled by dual specificity phosphatases (DSPases), but few inhibitors of Erk dephosphorylation have been identified. Using a high-content, fluorescence-based cellular assay and the National Cancer Institute's 1990 agent Diversity Set, we identified ten compounds (0.5%) that significantly increased phospho-Erk cytonuclear differences in intact cells. Three of the ten positive compounds inhibited the mitogen-activated protein kinase phosphatase-3 (MKP-3/PYST-1) in vitro without affecting VHR or PTP1B phosphatases. The most potent inhibitor of MKP-3 had an IC_{50} of <10 μM and inhibited MKP-3 in a novel, fluorescence-based multiparameter chemical complementation assay. These results suggest that the phospho-Erk nuclear accumulation assay may be a useful tool to discover DSPase inhibitors with biological activity.

Introduction

Dual-specificity phosphatases are intracellular enzymes that catalyze the removal of phosphate groups from threonine and tyrosine residues on the same protein substrate. Key enzymes that are tightly regulated by DSPases are the cyclin-dependent kinases, which are dephosphorylated by members of the Cdc25 family and control cell cycle progression, and mitogen-activated protein kinases (MAPK), which are dephosphorylated by MAPK phosphatases (MKPs) and have a pivotal role in mitogenic signal transduction, survival, stress response, and programmed cell death. The activation of MAPK pathways by upstream kinases and cell surface receptor-mediated events have been studied extensively. In contrast, the events that regulate termination of MAPK signaling are less well understood, although it is clear that MKPs play a major role [1]. There is also some evidence that activation of Erk, a member of the MAPK family, is regulated by the cell cycle phosphatase Cdc25A [2], possibly by affecting the tyrosine phosphorylation status and activity of Raf-1 [3]. A growing body of evidence suggests that prolonged activation of the Erk pathway can lead to cell cycle arrest [4] and cytotoxicity in several cell types, including human hepatoma cells [5]. Thus, inhibitors of phosphatases that dephosphorylate MAPK may exhibit growth inhibitory activity in cancer cells by perturbing the timing of Erk activation [2].

There is strong evidence for a role of DSPases in cancer. Members of the Cdc25 family were found overexpressed in a variety of human tumors (reviewed in [6]), and both Cdc25A and Cdc25B have oncogenic properties [7]. Evidence for an involvement of MKPs in oncogenesis comes from studies reporting overexpression of MKP-1 (CL-100) in prostate [8], breast [9], and ovarian cancer, where its expression level was also correlated with decreased progression-free survival [10]. Cell-active, selective DSPase inhibitors would therefore not only be valuable tools to help dissect the complex regulatory processes involved in the attenuation of Erk activation, but might also find applications as novel target-based antineoplastic therapies. While a few potent and selective Cdc25 inhibitors have been identified [11, 12], inhibitors of MKPs have not been reported to date.

Current efforts directed at phosphatase drug discovery encompass different strategies such as rational drug design [13] or in vitro chemical library screening on a larger scale [12]. Cell functions are, however, comprised of many interconnecting signaling and feedback pathways, and in vitro analyses based on isolated targets do not address this complexity. In addition, in vitro assays do not provide information about physicochemical parameters that determine whether a compound has the ability to penetrate cellular membranes. In contrast, target-based cellular assays would identify only those compounds that enter cells. Here we report for the first time the use of a high-content, cell-based assay in the discovery of cell-active DSPase inhibitors. We analyzed the NCI Diversity Set, which is a computationally selected subset of the NCI compound repository (described in [11]), for phospho-Erk nuclear accumulation as an endpoint consistent with inhibition of either Cdc25 or MKPs in intact cells. We found that compounds with Erk-activating activity were enriched for in vitro Cdc25 inhibitors. We then examined the selectivity of newly identified agents against Cdc25-related phosphatases and identified one compound that inhibited MKP-3 but not the protein tyrosine phosphatase PTP1B or the prototype DSPase VHR. Finally, we developed a novel multiparametric, fluorescence-based assay that specifically measured MKP-3 activity in intact cells and used it to demonstrate inhibition of MKP-3 in whole cells. The results demonstrate the utility of a target-based cellular screen for phospho-Erk nuclear accumulation as a tool in the discovery of cell-active DSPase inhibitors.

Results

Erk Activation by Submicromolar Cdc25 Inhibitors

Because we had previously shown that the Cdc25 inhibitor Compound 5 (NSC 672121) possessed Erk-activating activity [2], we asked whether Erk activation was a gen-

*Correspondence: lazo@pitt.edu

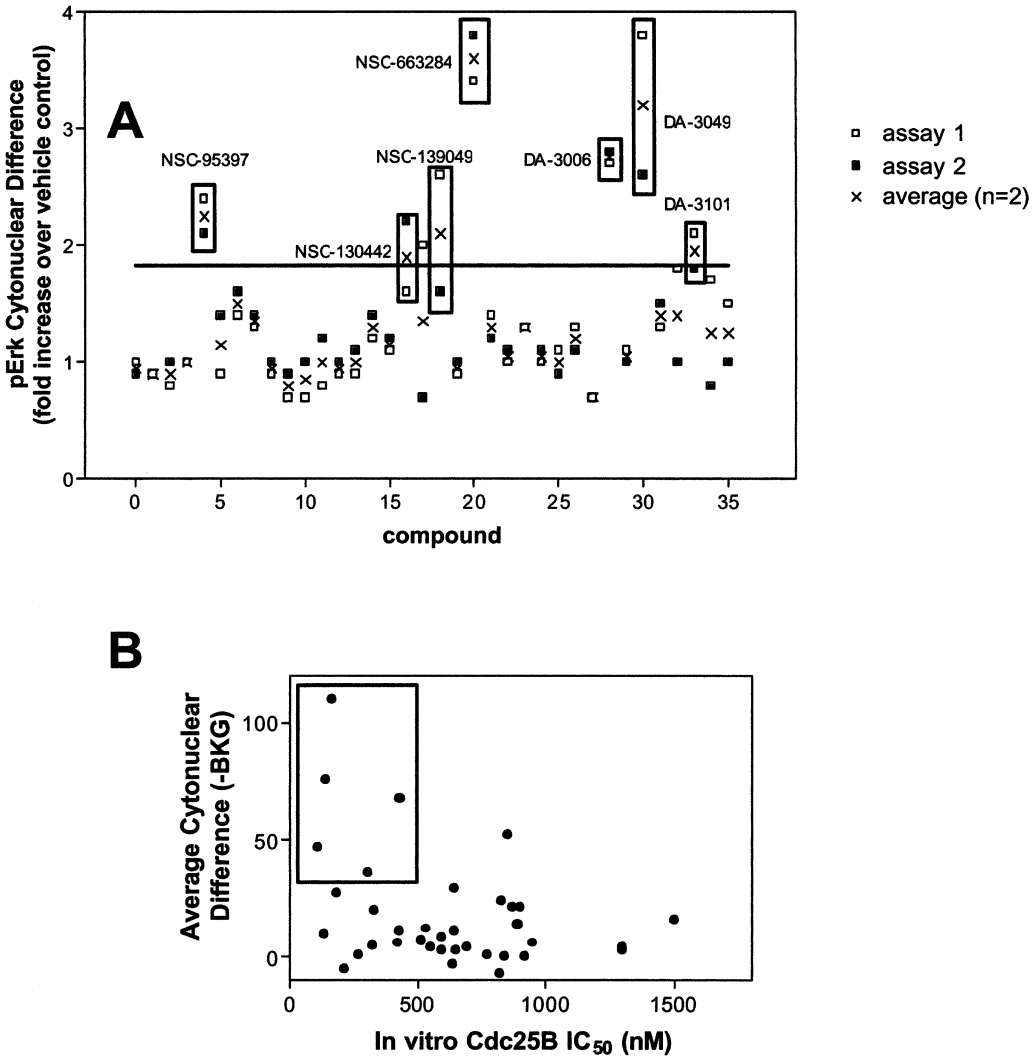

Figure 1. A Targeted Library of Cdc25 Inhibitors Is Enriched for Erk Activators

A focused library of 36 compounds with submicromolar activity against Cdc25B2 was analyzed for nuclear phospho-Erk accumulation on the ArrayScan II.

(A) Cytonuclear difference values from two individual multiwell plates (open and closed squares) were calculated for each compound. Compounds whose average cytonuclear difference values (crosses) were greater than 2-fold over vehicle control (solid line) were scored as positives. Seven compounds out of 36 (19.5%) were positives and are labeled with identifiers.

(B) Background-corrected cytonuclear difference values from wells treated with compounds at 10 μM were plotted against their IC_{50} values for Cdc25B2 inhibition. Five of the most active Cdc25 inhibitors were found in the top 30th percentile of Erk accumulators (boxed).

eral feature of compounds with Cdc25 inhibitory activity. Thirty-six agents, 22 of which were members of a previously evaluated 10,070 compound set from the NCI repository [12] plus 14 synthetic analogs, which we previously found were potent in vitro inhibitors of Cdc25 (IC_{50} values < 1 μM) [11, 12], were analyzed for nuclear phospho-Erk accumulation. NIH3T3 cells were treated in duplicate 96-well microplates for 20 min with compounds or vehicle, fixed, and stained with an anti-phospho-Erk antibody. Images were acquired on a Cellomics ArrayScan II, an automated batch image acquisition and analysis system, using the previously described nucleus-to-cytoplasm translocation algorithm [2]. Of the 36 compounds analyzed, seven (19.5%) had cytonuclear difference values greater than 2-fold over background (Figure 1A). Figure 1B shows that, while there was no direct correlation among the compounds' phospho-Erk accumulating ability and their inhibitory activity against Cdc25 in vitro, several of the most potent Erk activators were clustered in the top 30th percentile of in vitro Cdc25 inhibitory activity. We therefore hypothesized that phospho-Erk nuclear accumulation might be a surrogate endpoint for Cdc25 inhibition.

A High-Content Screen for Erk-Activating Compounds in Intact Mammalian Cells

We then examined the members of the publicly available NCI Diversity Set, a computationally selected subset

Table 1. Selection Statistics for Compounds that Caused Nuclear Accumulation of Phospho-Erk in Mammalian Cell-Based High-Content Screen

	Number of Compounds	
	% of Initial Positive Compounds	% of NCI Diversity Set
Total number of compounds		1990 (100%)
Positive compounds for phospho-Erk nuclear accumulation		34 (1.7%)[a]
Artifacts		24 (1.2%)
Rounding	5 (15%)	
Toxicity	8 (24%)	
Analysis	9 (26%)	
Autofluorescence	2 (6%)	
Remaining positive compounds	10 (29%)	10 (0.5%)
Microscopically confirmed	10 (29%)	
Bona fide number of positive compounds		10 (0.5%)

[a] Based on the average cytonuclear difference values from two independent experiments.

of the National Cancer Institute's compound repository [11], for their ability to increase nuclear accumulation of phosphorylated Erk in intact mammalian cells. Table 1 shows the selection statistics for compounds causing phospho-Erk nuclear accumulation. The vast majority of compounds did not affect Erk phosphorylation. Agents that caused a greater than 2-fold increase over the average cytonuclear differences from all 1990 compounds were scored as positives. Using these criteria, we identified 34 compounds as positive, an initial "hit rate" of 1.75%. Visual examination of the archived immunofluorescence images confirmed elevated nuclear phospho-Erk levels for ten of the initial positive compounds (not shown). The remaining 24 compounds were classified as artifacts of various types (Table 1). Thus, the bona fide percentage of positive compounds in the intact mammalian cell screen was 10/1990, or 0.5%.

An increase in cytonuclear difference values is indicative of Erk activation through phosphorylation, translocation, or both. We therefore examined the frequency distributions of cytonuclear and cytoring intensities in the entire cell population for each well to determine the relative contributions of cytoplasmic and nuclear fluorescence intensities to the cytonuclear difference values. Figure 2 shows that all compounds increased Erk phosphorylation in both the cytoplasm and in the nucleus. While most compounds caused a more pronounced increase in nuclear pErk, some of them showed similar increases in cytoplasmic and nuclear phospho-Erk intensities. Thus, the increases in phospho-Erk cytonuclear difference values caused by some compounds were not exclusively due to protein translocation, but resulted from an increase in overall phospho-Erk levels.

In Vitro Phosphatase Inhibition Studies

MKP-3, Cdc25A, and VHR have been reported to mediate Erk dephosphorylation. Therefore, we analyzed all positive compounds for in vitro inhibition of MKP-3, Cdc25A, VHR, and the tyrosine phosphatase PTP1B. At the highest concentration tested (10 μM), three compounds (NSC 45382, NSC 295642, and NSC 357756) inhibited MKP-3 (PYST-1) by 50% or more, and three (NSC 310551, NSC 295642, and NSC 321206) inhibited the catalytic domain of Cdc25A (Table 2). None of the compounds showed significant inhibition of full-length Cdc25B, but two (NSC 295642 and NSC 321206) were active against a truncated form of Cdc25B lacking the regulatory N terminus. All compounds were devoid of activity against the prototype DSPase, VHR, or the protein tyrosine phosphatase, PTP1B. The most active compound against MKP-3, NSC 357756, inhibited MKP-3 with an IC_{50} of 8.0 μM and appeared to be selective for MKP-3 over all other phosphatases tested. Western blot analysis on whole-cell lysates from cells treated with compounds that had antiphosphatase activity confirmed the results from the immunofluorescence-based screen. Figure 3 shows that the five compounds that inhibited either MKP-3, Cdc25A, or both caused an increase in total cellular Erk phosphorylation that was comparable

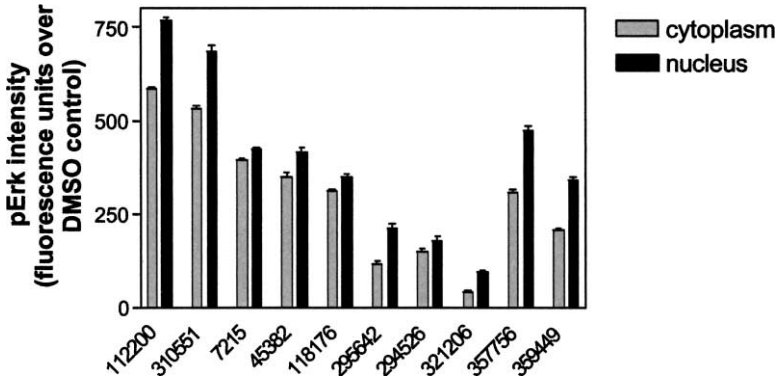

Figure 2. Relative Changes in Cytoplasmic versus Nuclear pErk Levels in Cells Treated with Visually Confirmed Positive Compounds in the NCI Diversity Set

Nuclear and cytoplasmic phospho-Erk intensities were retrieved from archived image analysis data for all ten positive compounds from the phospho-Erk nuclear accumulation screen. All positive compounds caused both an increase in cytoplasmic and in nuclear phospho-Erk intensity. Data are the average cytoplasmic (hatched) or nuclear (solid bars) intensities of 326 to 560 cells ± SEM and presented as the average fluorescence intensity increase over vehicle-treated control.

Table 2. In Vitro Phosphatase Inhibition by Erk Activators

	Percent Inhibition at 10 μM					
NSC	MKP-3[a,b]	Cdc25B[a,b]	Cdc25A[b,c]	Cdc25B[b,c]	VHR[d]	PTP1B[d]
112200	inactive	inactive	47 ± 3	inactive	inactive	inactive
310551	15 ± 3	18 ± 2	54 ± 43	12 ± 3	inactive	inactive
7215	33 ± 6	22 ± 4	49 ± 4	inactive	inactive	inactive
45382	53 ± 6	28 ± 15	36 ± 4	inactive	inactive	inactive
118176	13 ± 3	23 ± 8	32 ± 4	inactive	inactive	inactive
295642	50 ± 3	21 ± 8	74 ± 2	61 ± 7	inactive	inactive
294526	inactive	inactive	35 ± 4	inactive	inactive	inactive
321206	45 ± 4	36 ± 6	72 ± 6	87 ± 3	inactive	inactive
357756	64 ± 4	20 ± 7	inactive	19 ± 4	inactive	inactive
359449	inactive	inactive	21 ± 6	inactive	inactive	inactive

Inactive indicates less than 10% inhibition.
[a] Full-length His_6-tagged protein.
[b] Minimum of three independent determinations ± SD.
[c] Catalytic domain.
[d] Full-length GST fusion protein.

to or greater than that of the previously described Cdc25 inhibitor, Compound 5 (NSC 672121).

Structural Comparisons

Figure 4 shows the structures of Erk-activating compounds. Two of the ten positive compounds were quinones, one of them (NSC 45382) being closely related to NSC 663284, one of the two most potent in vitro Cdc25 inhibitors described to date [11], thereby validating the quinone structure as a pharmacophore for Cdc25 inhibition. Four compounds were transition metal complexes, among them the two compounds (NSC 295642 and NSC 321206) that possessed the highest Cdc25A inhibitory activity. The most active MKP-3 inhibitor, NSC 357756, was structurally unrelated to any of the other compounds.

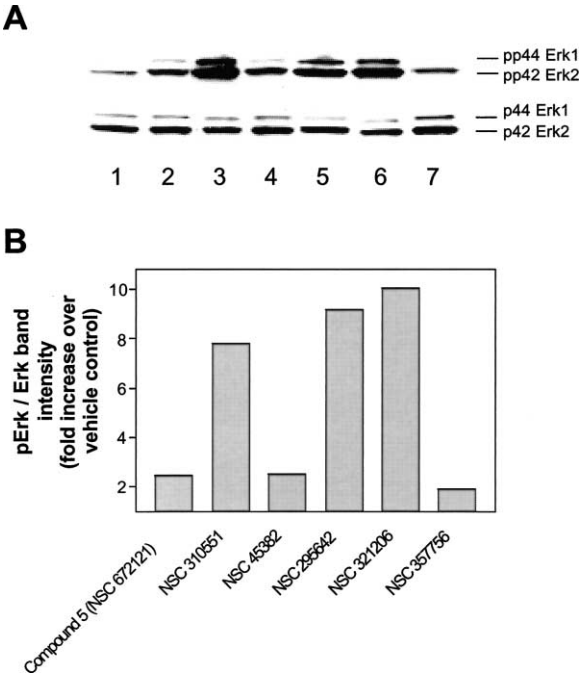

Figure 3. Western Blot Analysis for Phosphorylated Erk in Compounds with Anti-MKP-3 or Cdc25A Activity

(A) Cells were treated with 10 μM of compounds or vehicle for 20 min and lysed, and lysates were immunoblotted with anti-phospho-Erk or anti-Erk antibodies, respectively.

(B) Phospho-Erk bands were scanned by densitometry and intensities normalized to total Erk. Data are from a single experiment that has been repeated with similar results and are presented as fold increase over vehicle control. Lane 1, DMSO (vehicle); lanes 2–7, Compound 5 (NSC 672121), NSC 350551, NSC 45382, NSC 295642, NSC 321206, and NSC 357756, respectively.

NSC 357756 Inhibits MKP-3 in Whole Cells

Because of the lack of confirmed MKP-3 inhibitors, we developed a multiparameter fluorescence-based cellular assay based on our previously described "chemical complementation" strategy [2] to determine whether NSC 357756 was able to inhibit MKP-3 in intact cells. HeLa cells were transfected with a c-*myc*-tagged version of MKP-3 and stimulated with 12-O-tetradecanoylphorbol 13-acetate (TPA) to generate a strong phospho-Erk signal that was distributed as uniformly as possible throughout the entire cell population. Cells were then stained simultaneously with anti-phospho-Erk and anti-c-*myc* antibodies, followed by Alexa 546- and Alexa 488-conjugated secondary antibodies to visualize phospho-Erk and c-*myc*-MKP-3, respectively. Fluorescence images acquired with TRITC and FITC compatible filter sets revealed that none of the MKP-3-expressing cells responded to TPA with increased Erk phosphorylation (Figure 5A). Expression of the phosphatase-inactive green fluorescent protein (GFP) did not affect the cells' responsiveness to TPA (data not shown). Inclusion of the broad-spectrum PTPase inhibitor, phenylarsine oxide (PAO, 50 μM), completely restored responsiveness to TPA in MKP-3-expressing cells (Figure 5B). PAO (10 μM) and NSC 357756 (10 μM) partially reversed the MKP-3-induced loss of phospho-Erk in the cells that stained positive for MKP-3 (Figures 5C and 5D).

c-*myc*-MKP-3 (FITC) and pErk (TRITC) levels were then quantitated in approximately 4000 individual cells by automated image analysis on the ArrayScan II. First, the number of MKP-3 expressors was determined for

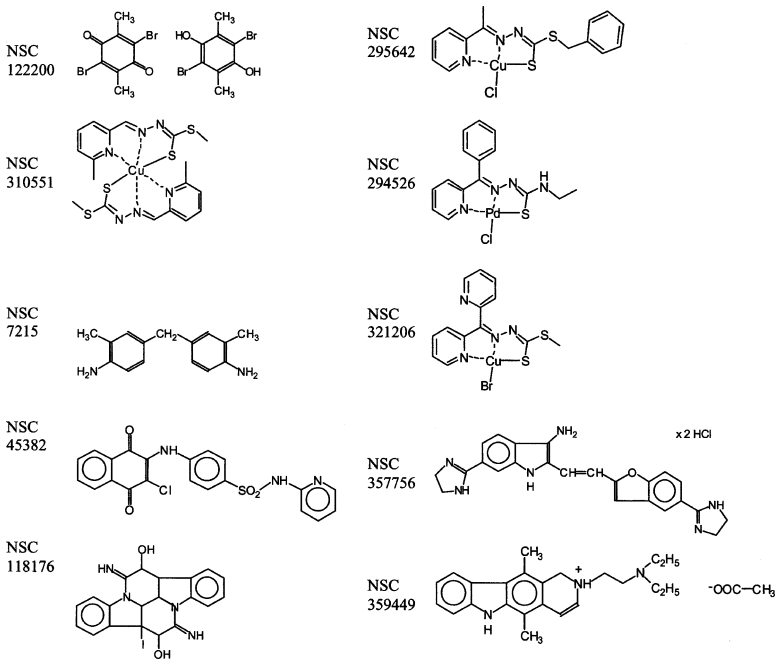

Figure 4. Structures of Erk Activators from the Cell-Based Screen

each condition by choosing appropriate intensity cutoff values from FITC (Alexa 488) intensity distribution histograms. Based on this method, we found transfection efficiencies of 6% to 23% for MKP-3 and 53% for GFP. We then determined average nuclear phospho-Erk intensities in the two cell subpopulations. Figure 6 shows the differences in nuclear phospho-Erk intensities between cell subpopulations that did or did not express MKP-3 or GFP. We found that in GFP-expressing cells, there was little difference in phospho-Erk levels after TPA stimulation whether cells expressed GFP or not (Figure 6). The small increase in phospho-Erk intensities in GFP-expressing cells, which manifested itself as a negative difference between the two cell populations, was due to spectral overlap between the two fluorophores. In contrast, cells transfected with MKP-3 and treated with TPA showed significantly lower levels of nuclear phospho-Erk specifically in the MKP-3 expressing cells (Figure 6), consistent with the images shown in Figure 5A. The broad spectrum PTPase inhibitor, phenylarsine oxide (PAO), restored responsiveness to TPA in MKP-3-expressing cells as evidenced by a concentration-dependent decrement in pErk differences between MKP-3 expressing and nonexpressing subpopulations, indicating that PAO inhibited MKP-3 in the cell. A concentration of 50 μM PAO reduced pErk level differences to those seen in cells transfected with GFP. Inclusion of the putative MKP-3 inhibitor, NSC 357756, resulted in a partial rescue of TPA responsiveness that was comparable in magnitude to that seen with 5 to 10 μM PAO.

NSC 357756 Has Antitumor Activity In Vivo

In vivo antitumor data against a variety of tumors have been generated by the National Cancer Institute for many of the compounds in the NCI compound repository [14]. These results are publicly available on the Developmental Therapeutics Program website (http://dtp.nci.nih.gov/webdata.html). We therefore mined the NCI's web-accessible database for antitumor activity in mice using the compounds that were positive for phospho-Erk nuclear accumulation. Using an increased survival time of 135% over untreated control (T/C $>$ 135%) as an accepted standard for significant antitumor activity, we found that NSC 357756 had activity against P388 leukemia (T/C $=$ 139% at 25 mg/kg/dose, 6/6 animals surviving), L1210 leukemia (T/C $=$ 178% at 18 mg/kg/dose, 6/6 animals surviving), and M5076 sarcoma (T/C $=$ 137% at 50 mg/kg/dose, 8/10 animals surviving). A second positive compound from the screen, namely NSC 295642, had activity against P388 leukemia (T/C $=$ 136% at 3.12 mg/kg/dose, 6/6 animals surviving).

Discussion

Advances in genomics research, combinatorial chemistry, and laboratory automation have made it possible to interrogate large compound collections in a short period of time. High-throughput screening has therefore become a main component of contemporary drug discovery. The vast majority of these screens are based on in vitro assays, which have the advantage of being ultra-high-throughput but do not take into consideration other parameters, for example, physicochemical properties that determine drug-like behavior such as cell permeability. Furthermore, target-based screening assays may not be predictive of drug effect within the context of the whole cell [15]. Thus, attempts have been made to incorporate cell-based screens into the early stages of the drug discovery process to select for compounds with cellular activity. Examples include screening of yeast strains for DNA damaging agents [16], A-549 lung cancer cells for inhibitors of motor proteins by Western

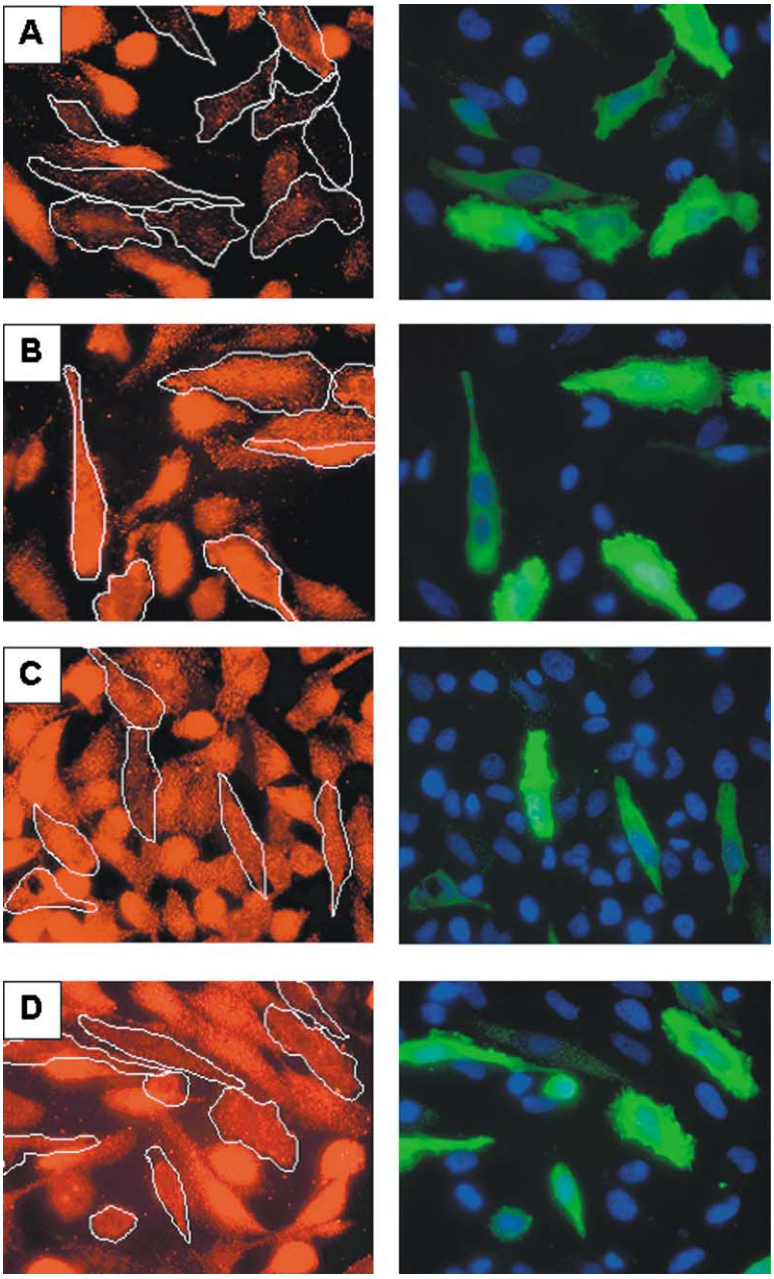

Figure 5. A Fluorescence-Based Chemical Complementation Assay

HeLa cells were transfected in 384-well plates with cDNAs encoding c-*myc*-tagged MKP-3 as described in Experimental Procedures. Twenty-four hours after transfection, cells were treated for 15 min with TPA (500 ng/ml) in the absence or presence of phenylarsine oxide (PAO) or NSC 357756 and immunostained with anti-c-*myc* and anti-phospho-Erk antibodies. Nuclei were counterstained with Hoechst 33342. Right, nuclei and MKP-3; left, phospho-Erk.

(A) TPA only, (B) 50 μM PAO, (C) 10 μM PAO, (D) 10 μM NSC 357756.

blot analysis of phospho-nucleolin [17], and a morphological differentiation screen in C2C12 muscle cells for tubulin disrupting agents [18]. Most of these screens are single-parameter phenotypic assays in whole cell populations.

High-content screening is a recently introduced analysis tool designed to yield information about the activity and spatial regulation of multiple targets in individual cells rather than in a cell population as a whole [19, 20]. Due to the novelty of this concept, a shortage of suitable assays, and the instrumentation necessary to perform them in a high-throughput format, however, little information exists in the literature about the outcomes of high-content drug discovery screens in intact mammalian cells.

Here we have for the first time investigated the utility of a target-based cellular screen to identify compounds that caused nuclear accumulation of phosphorylated Erk. Based on the well-established role for MKPs in Erk deactivation [1] and on our previously published observation that ectopic expression of Cdc25A caused a decrease in Erk phosphorylation [2], we hypothesized that nuclear phospho-Erk accumulation would represent a suitable intracellular target marker for compounds with dual-specificity phosphatase activity. Using the previously described nuclear translocation assay on an Cellomics ArrayScan II solid-phase cytometer [2, 21], we obtained information about both Erk phosphorylation status and subcellular localization after short-term treatment of NIH3T3 cells with the NCI Diversity Set, a pre-

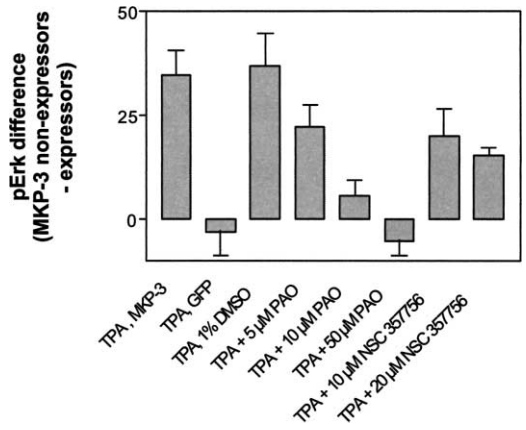

Figure 6. Quantitation of Nuclear Phospho-Erk Levels in MKP-3 Expressing and Nonexpressing Cell Subpopulations

The identical 384-well plate described in the legend to Figure 5 was scanned at excitation/emission wavelengths of 350/461 nm (Hoechst), 494/519 nm (Alexa 488), and 556/573 nm (Alexa 546) on the ArrayScan II using the general screening application. Approximately 1000 individual cells from each well were simultaneously analyzed for phospho-Erk, c-*myc*-MKP-3, and GFP intensities. Cells were separated into MKP-3 (GFP) expressing and nonexpressing subpopulations by setting appropriate gates in the FITC (Alexa 488) channel, and average nuclear phospho-Erk intensities were calculated for MKP-3 (GFP) expressors and nonexpressors. Bars represent the average difference in nuclear phospho-Erk intensities between nonexpressing and MKP-3 (GFP)-expressing subpopulations from quadruplicate wells. Data are from a single experiment that has been repeated with similar results.

viously described compound library selected for maximal chemical diversity. This screen identified ten compounds as positives, a 0.5% "hit rate."

In vitro phosphatase studies using recombinant proteins and the small molecule substrate OMFP revealed that, of the ten positive compounds identified from the screen, three (30%) inhibited MKP-3 by more than 50% at 10 μM. Three compounds had activity against Cdc25A catalytic domain. The most potent inhibitor of MKP-3, NSC 357756, had an IC_{50} of 8.0 μM, making it the first low micromolar MKP-3 inhibitor reported to date. None of the positives inhibited VHR, which has also been reported to dephosphorylate Erk [22]. This was of interest because the active site in all DSPases and in PTPases has the same signature motif [23] and because VHR is a prototype DSPase that has substantial similarity to both Cdc25 [24] and MKP-3 [25]. These data suggest that it may be possible to generate selective inhibitors of these highly related enzymes.

The investigation of whether NSC 357756 had the ability to inhibit MKP-3 in whole cells necessitated the development of a novel assay system for cellular MKP-3 activity. The phosphorylation status of proteins is directly controlled by kinase and phosphatase activities, but other factors, such as growth factors, cytokines, or cellular stress, also influence protein phosphorylation levels. In addition, many proteins are subject to activation and deactivation by multiple kinases and phosphatases. For example, Erk dephosphorylation has been described for a number of MAPK phosphatases and the serine/threonine phosphatase, PP2A. Thus, while protein phosphorylation levels, even when measured on specific target proteins, are a readout consistent with an alteration in either kinase or phosphatase activity, they do not yield information about target specificity.

We therefore devised a fluorescence-based, multiparametric variant of our previously described chemical complementation assay [2, 11] to confirm that NSC 357756 inhibited MKP-3 in whole cells. This assay is based on the selective measurement of Erk phosphorylation in MKP-3 expressing and nonexpressing cell subpopulations in the presence or absence of the compound of interest. Immunofluorescence images presented by Brunet et al. [26] had indicated that MKP-3 expressing CCL-39 cells did not respond to serum stimulation with enhanced Erk phosphorylation. Consistent with their data, we found that, in a transiently transfected and TPA-stimulated HeLa cell population, cells that expressed MKP-3 appeared to have significantly lower pErk levels than those not expressing MKP-3. We then used automated batch image acquisition and analysis to simultaneously quantitate MKP-3 expression and nuclear phospho-Erk levels in approximately 4000 individual cells. Cells were gated into expressing or nonexpressing cell subpopulations based on MKP-3 label intensity, and phospho-Erk intensities were averaged from both subpopulations. We found that there was a consistent, quantifiable, and significant difference in phospho-Erk levels in cells that did or did not express MKP-3. In contrast, cells expressing phosphatase-inactive GFP had phospho-Erk levels similar to or higher than cells not expressing GFP. The difference in nuclear phospho-Erk intensities between the two subpopulations was fully abrogated in the presence of 50 μM phenylarsine oxide, and partially abrogated in the presence of 10 μM and 20 μM NSC 357756, indicating that NSC 357756 had the ability to inhibit MKP-3 in the cell. We are currently expanding the scope of this assay to investigate whether NSC 357756 inhibits other MKPs or the various Cdc25 isoforms.

By choosing the NCI Diversity Set, we exploited substantial information readily available from the NCI Developmental Therapeutics Program about the in vivo antitumor activity of this library against various tumors. Antitumor data in a variety of mouse models have been archived for seven of the ten positives identified in the phospho-Erk accumulation screen. Of these seven compounds, two had significant activity against at least one tumor type. In contrast, among 14 submicromolar inhibitors of Cdc25, which were identified from a much larger subset of the NCI compound repository [12], none had activity in vivo. Although the sample size we are analyzing is small, the data are consistent with the notion that cell-based screens may be biased toward the identification of biologically active agents. It is also interesting to note that we did not identify the most active compound, NSC 357756, as an active compound from the in vitro screen in our previous studies [11, 12], because it was not a submicromolar in vitro inhibitor of Cdc25. Thus, the cell-based assay detected a compound that was active in whole cells, even though it was not one of the most potent inhibitors of Cdc25 or MKP-3. The data suggest that both approaches, namely in vitro high-throughput screening and target-based cellular assays,

should be used as complementary prioritization tools in the early drug discovery process.

Significance

High-throughput screening has become a main component of contemporary drug discovery. Many of the high-throughput screens used today are based on in vitro assays, which have the advantage of being ultra-high-throughput but do not take into consideration other parameters, for example, physicochemical properties that determine drug-like behavior such as cell permeability. Furthermore, target-based screening assays may not be predictive of drug effect within the context of the whole cell. We therefore investigated the utility of a cell-based, high-content screening process, which generated information about the content and spatial regulation of multiple macromolecules in individual cells, to select for compounds with cellular activity. We chose as targets dual-specificity phosphatases (DSPases), which have a critical role in the regulation of many signaling pathways including mitogen-activated protein kinase (MAPK) and cyclin-dependent kinase (Cdk) activation. Several DSPases have been shown to have oncogenic properties, but small molecule inhibitors of DSPases with cellular activity are lacking. We analyzed the NCI Diversity Set, a chemically diverse compound library, for phospho-Erk nuclear accumulation in intact mammalian cells, followed by in vitro analysis of antiphosphatase activity using recombinant enzymes. The assay enriched substantially for in vitro phosphatase inhibitors. One compound, namely NSC 357756, inhibited the Erk-specific DSPase MKP-3 both in vitro and in a newly developed multiparameter fluorescence-based assay designed to specifically measure MKP-3 inhibition in intact cells. Furthermore, NSC 357756 had in vivo antitumor activity in a variety of mouse models. The data suggest that a cellular assay for Erk phosphorylation, coupled with a chemical complementation strategy, may be a powerful tool in the discovery of lead structures for novel, cell-active DSPase inhibitors.

Experimental Procedures

Reagents

Compound 5 (NSC 672121, (2-(2-mercaptoethanol)-3-methyl-1,4-naphthoquinone) has been described previously [27]. The NCI Diversity Set was provided by Daniel W. Zaharevitz (National Cancer Institute, Rockville, MD) and has been described elsewhere [11]. Mouse monoclonal anti-phospho-Erk (E10), rabbit polyclonal phospho-Erk, and rabbit polyclonal pan-Erk antibodies were from Cell Signaling Technology (Beverly, MA). Secondary antibodies were Alexa Fluor 488-conjugated goat anti-mouse, Alexa Fluor 546-conjugated goat anti-rabbit IgG (Molecular Probes, Eugene, OR), and HRP-conjugated goat anti-rabbit IgG and goat-anti mouse IgG (Jackson ImmunoResearch, West Grove, PA). cDNA encoding myc-tagged MKP-3 (PYST-1) in a pSG5 mammalian expression vector [28, 29] was a gift from Dr. Stephen Keyse (IRCF, Dundee, UK). The bacterial expression vector for His_6-MKP-3 was a gift from Dr. Zhong-Yin Zhang (Albert Einstein College of Medicine, Bronx, NY). The pEGFP-C1 expression vector was from Clontech (Palo Alto, CA).

Cell Culture

NIH 3T3 and HeLa cells were obtained from ATCC (Manassas, VA) and were maintained in Dulbecco's Minimum Essential Medium (DMEM) containing 10% fetal bovine serum (FBS, HyClone, Logan, UT) and 1% penicillin-streptomycin (Life Technologies, Inc., Rockville, MD) in a humidified atmosphere of 5% CO_2 at 37°C.

Cell-Based Screen

NIH 3T3 cells (2000 cells per well) were plated in the wells of collagen-coated 96-well darkwell plates (Packard ViewPlate) and allowed to attach overnight. Cells were treated for 20 min with compounds, fixed with 3.7% formaldehyde in PBS, and permeabilized with PBS/Triton X-100. Cells were stained with Hoechst 33342 fluorescent dye to visualize nuclei. Phospho-Erk immunoreactive cells were visualized by staining with a phospho-specific Erk antibody followed by an Alexa Fluor 488-conjugated secondary antibody (Molecular Probes, Eugene, OR) using an XF100 filter set at excitation/emission wavelengths of 494/519 nm (Alexa 488) and 350/461 nm (Hoechst), respectively. Plates were analyzed by automated image analysis on the ArrayScan II system (Cellomics, Pittsburgh, PA) using the previously described cytoplasm-to-nuclear translocation algorithm [2, 21]. The algorithm is based on measurements of phospho-Erk fluorescence intensity within a nuclear mask defined by Hoechst 33342 staining (referred to as "cytonuclear intensity") and within a cytoplasmic region defined by a set of concentric circles placed around the nuclear mask (referred to as "cytoring intensity") [21]. Both cytonuclear and cytoring intensities were normalized to the total cytonuclear or cytoring area and expressed as average intensity per pixel. Cytoplasmic-to-nuclear difference values were calculated by subtracting the average cytoring intensity per pixel from the average cytonuclear intensity per pixel.

Compounds were analyzed as single data points on two separate plates. Each plate contained negative control wells that did not receive primary antibody, four wells treated with vehicle alone, and four wells treated with Compound 5 (NSC 672121, 10 μM) as a positive internal control.

Western Blotting

NIH 3T3 cells were plated in 100 mm tissue culture dishes, exposed to compounds for 20 min, harvested by trypsinization, and lysed. Cell lysates were resolved on 4%–20% SDS-PAGE gels and transferred to nitrocellulose membranes (Protran, Schleicher & Schuell, Keene, NH). Membranes were probed with anti-phospho-Erk and anti-Erk antibodies. Positive antibody reactions were visualized using peroxidase-conjugated secondary antibodies (Jackson ImmunoResearch, West Grove, PA) and an enhanced chemiluminescence detection system (Renaissance, NEN, Boston, MA) according to manufacturer's instructions. For quantitation of protein expression levels, X-ray films were scanned on a Molecular Dynamics personal SI densitometer and analyzed using the ImageQuant software package (Ver. 4.1, Molecular Dynamics, Sunnyvale, CA).

In Vitro Phosphatase Assays

Full-length MKP-3 and Cdc25B2 were expressed as His_6-tagged fusion proteins from a pET21a vector. The catalytic domain of Cdc25A (amino acids 336–523) was subcloned into a pET21a vector as previously described [30]. Full-length VHR and PTP1B were expressed as GST fusion proteins from a pGEX2T vector as described [31]. GST and His_6-tagged fusion proteins were purified from *E. coli* using standard methodology. Phosphatase inhibition studies were performed using a fluorescence-based 96-well microtiter plate assay with O-methyl fluorescein diphosphate (OMFP) as previously described [11, 31].

Analysis of Phospho-Erk Levels in MKP-3 Expressing and Nonexpressing HeLa Cell Subpopulations

HeLa cells (5000) were plated in the wells of a collagen-coated 384-well plate (Falcon Biocoat) and allowed to attach overnight. Cells were transfected with MKP-3 or EGFP cDNAs (100 ng/well) and Lipofectamine 2000 (Invitrogen, Carlsbad, CA; 1 μl per 0.4 μg DNA) in OPTIMem reduced serum medium as per manufacturer's instructions. Four hours after transfection, complexes were removed and fresh medium containing 10% FBS was added. Eighteen hours later, cells were treated in quadruplicate wells for 15 min with TPA or mixtures of TPA and phosphatase inhibitors, fixed, and immunostained with a mixture of anti-phospho-Erk (1:200 dilution, Cell Sig-

naling Technology, Beverly, MA) and anti-c-*myc* (1:100 dilution, Santa Cruz Biotechnology, Santa Cruz, CA) antibodies as described above except that a 1 hr blocking step in PBS containing 10% goat serum and 1% BSA was included before addition of primary antibodies. Positive phospho-Erk and c-*myc*-MKP-3 signals were visualized with Alexa-546 (phospho-Erk) and Alexa-488 (c-*myc*)-conjugated secondary antibodies, respectively. Control conditions omitting Alexa-546 secondary antibody were included on each plate to assess nonspecific phospho-Erk background staining. All staining steps were carried out on a Biomek 2000 laboratory automation workstation (Beckman-Coulter, Inc., Fullerton, CA).

Plates were analyzed by three-channel multiparametric analysis for phospho-Erk and c-*myc*-MKP-3 intensities in an area defined by nuclear staining using the general screening application on the ArrayScan II (Cellomics, Pittsburgh, PA). Images were acquired in three independent channels using an Omega XF57 filter set at excitation/emission wavelengths of 350/461 nm (Hoechst), 494/519 nm (Alexa 488), and 556/573 nm (Alexa 546). Approximately 4000 individual cells were analyzed for phospho-Erk and c-*myc*-MKP-3 or GFP intensities. For each condition, the percentage of MKP-3 (GFP)-expressing cells was determined from FITC (Alexa-488) intensity distribution histograms, setting appropriate gates for MKP-3 (GFP)-positive and MKP-3 (GFP)-negative cells. Phospho-Erk levels were then averaged in MKP-3 expressing and nonexpressing subpopulations. Large positive differences in phospho-Erk intensities between the two subpopulations indicated lower levels of phospho-Erk in MKP-3-expressing cells compared with nonexpressing cells. Low differences indicated similar levels of phospho-Erk in both cell subpopulations. Negative differences were a result of spectral overlap between the two fluorophores, resulting in an elevated background signal in the red channel caused by green fluorescence emission.

Acknowledgments

We thank Dr. Stephen Keyse and Dr. Zhong-Yin Zhang for providing MKP-3 expression plasmids, Dr. Daniel Zaharevitz for a critical review of the manuscript, and John Skoko for technical assistance. This work was supported in part by NIH grants CA78039 and CA52995 and by the Fiske Drug Discovery Fund.

The University of Pittsburgh requires that the authors disclose to the readers that J.S. Lazo is on the Scientific Advisory Board of Cellomics, Inc., and, therefore, has a small financial interest in the company. Cellomics did not support this research or provide any funds for these studies.

Received: May 7, 2003
Revised: June 16, 2003
Accepted: June 23, 2003
Published: August 22, 2003

References

1. Keyse, S.M. (2000). Protein phosphatases and the regulation of mitogen-activated protein kinase signalling. Curr. Opin. Cell Biol. *12*, 186–192.
2. Vogt, A., Takahito, A., Ducruet, A.P., Chesebrough, J., Nemoto, K., Carr, B.I., and Lazo, J.S. (2001). Spatial analysis of key signaling proteins by high-content solid-phase cytometry in Hep3B cells treated with an inhibitor of Cdc25 dual-specificity phosphatases. J. Biol. Chem. *276*, 20544–20550.
3. Xia, K., Lee, R.S., Narsimhan, R.P., Mukhopadhyay, N.K., Neel, B.G., and Roberts, T.M. (1999). Tyrosine phosphorylation of the proto-oncoprotein Raf-1 is regulated by Raf-1 itself and the phosphatase Cdc25A. Mol. Cell. Biol. *19*, 4819–4824.
4. Pumiglia, K.M., and Decker, S.J. (1997). Cell cycle arrest mediated by the MEK/mitogen-activated protein kinase pathway. Proc. Natl. Acad. Sci. USA *94*, 448–452.
5. Nishikawa, Y., Wang, Z., Kerns, J., Wilcox, C.S., and Carr, B.I. (1999). Inhibition of hepatoma cell growth in vitro by arylating and non-arylating K vitamin analogs. Significance of protein tyrosine phosphatase inhibition. J. Biol. Chem. *274*, 34803–34810.
6. Lyon, M.A., Ducruet, A.P., Wipf, P., and Lazo, J.S. (2002). Dual-specificity phosphatases as targets for antineoplastic agents. Nat. Rev. Drug Discov. *1*, 961–976.
7. Galaktionov, K., Lee, A.K., Eckstein, J., Draetta, G., Meckler, J., Loda, M., and Beach, D. (1995). CDC25 phosphatases as potential human oncogenes. Science *269*, 1575–1577.
8. Magi-Galluzzi, C., Mishra, R., Fiorentino, M., Montironi, R., Yao, H., Capodieci, P., Wishnow, K., Kaplan, I., Stork, P.J., and Loda, M. (1997). Mitogen-activated protein kinase phosphatase 1 is overexpressed in prostate cancers and is inversely related to apoptosis. Lab. Invest. *76*, 37–51.
9. Wang, H., Cheng, Z., and Malbon, C.C. (2003). Overexpression of mitogen-activated protein kinase phosphatases MKP1, MKP2 in human breast cancer. Cancer Lett. *191*, 229–237.
10. Denkert, C., Schmitt, W.D., Berger, S., Reles, A., Pest, S., Siegert, A., Lichtenegger, W., Dietel, M., and Hauptmann, S. (2002). Expression of mitogen-activated protein kinase phosphatase-1 (MKP-1) in primary human ovarian carcinoma. Int. J. Cancer *102*, 507–513.
11. Lazo, J.S., Aslan, D.C., Southwick, E.C., Cooley, K.A., Ducruet, A.P., Joo, B., Vogt, A., and Wipf, P. (2001). Discovery and biological evaluation of a new family of potent inhibitors of the dual specificity protein phosphatase Cdc25. J. Med. Chem. *44*, 4042–4049.
12. Lazo, J.S., Nemoto, K., Pestell, K.E., Cooley, K., Southwick, E.C., Mitchell, D.A., Furey, W., Gussio, R., Zaharevitz, D.W., Joo, B., et al. (2002). Identification of a potent and selective pharmacophore for Cdc25 dual specificity phosphatase inhibitors. Mol. Pharmacol. *61*, 720–728.
13. Taing, M., Keng, Y.F., Shen, K., Wu, L., Lawrence, D.S., and Zhang, Z.Y. (1999). Potent and highly selective inhibitors of the protein tyrosine phosphatase 1B. Biochemistry *38*, 3793–3803.
14. Geran, R.I., Greenberg, N.H., Macdonald, M.M., Schumacher, A.M., and Abott, B.J. (1972). Protocols for screening chemical agents and natural products against animal tumors and other biological systems. Cancer Chemother. Rep. *3*, 1–95.
15. Balis, F.M. (2002). Evolution of anticancer drug discovery and the role of cell-based screening. J. Natl. Cancer Inst. *94*, 78–79.
16. Dunstan, H.M., Ludlow, C., Goehle, S., Cronk, M., Szankasi, P., Evans, D.R., Simon, J.A., and Lamb, J.R. (2002). Cell-based assays for identification of novel double-strand break-inducing agents. J. Natl. Cancer Inst. *94*, 88–94.
17. Mayer, T.U., Kapoor, T.M., Haggarty, S.J., King, R.W., Schreiber, S.L., and Mitchison, T.J. (1999). Small molecule inhibitor of mitotic spindle bipolarity identified in a phenotype-based screen. Science *286*, 971–974.
18. Rosania, G.R., Chang, Y.T., Perez, O., Sutherlin, D., Dong, H., Lockhart, D.J., and Schultz, P.G. (2000). Myoseverin, a microtubule-binding molecule with novel cellular effects. Nat. Biotechnol. *18*, 304–308.
19. Giuliano, K.A., DeBiasio, R.L., Dunlay, T., Gough, A., Volosky, J.M., Zock, J., Pavlakis, G.N., and Taylor, D.L. (1997). High-content screening: a new aproach to easing key bottlenecks in the drug discovery process. J. Biomol. Screen. *2*, 249–259.
20. Taylor, D.L., Woo, E.S., and Giuliano, K.A. (2001). Real-time molecular and cellular analysis: the new frontier of drug discovery. Curr. Opin. Biotechnol. *12*, 75–81.
21. Ding, G.J., Fischer, P.A., Boltz, R.C., Schmidt, J.A., Colaianne, J.J., Gough, A., Rubin, R.A., and Miller, D.K. (1998). Characterization and quantitation of NF-kappaB nuclear translocation induced by interleukin-1 and tumor necrosis factor-alpha. Development and use of a high capacity fluorescence cytometric system. J. Biol. Chem. *273*, 28897–28905.
22. Todd, J.L., Tanner, K.G., and Denu, J.M. (1999). Extracellular regulated kinases (ERK) 1 and ERK2 are authentic substrates for the dual-specificity protein-tyrosine phosphatase VHR. A novel role in down-regulating the ERK pathway. J. Biol. Chem. *274*, 13271–13280.
23. Tonks, N.K., and Neel, B.G. (1996). From form to function: signaling by protein tyrosine phosphatases. Cell *87*, 365–368.
24. Denu, J.M., Zhou, G., Wu, L., Zhao, R., Yuvaniyama, J., Saper, M.A., and Dixon, J.E. (1995). The purification and characterization of a human dual-specific protein tyrosine phosphatase. J. Biol. Chem. *270*, 3796–3803.
25. Stewart, A.E., Dowd, S., Keyse, S.M., and McDonald, N.Q.

(1999). Crystal structure of the MAPK phosphatase Pyst1 catalytic domain and implications for regulated activation. Nat. Struct. Biol. *6*, 174–181.

26. Brunet, A., Roux, D., Lenormand, P., Dowd, S., Keyse, S., and Pouyssegur, J. (1999). Nuclear translocation of p42/p44 mitogen-activated protein kinase is required for growth factor-induced gene expression and cell cycle entry. EMBO J. *18*, 664–674.
27. Nishikawa, Y., Carr, B.I., Wang, M., Kar, S., Finn, F., Dowd, P., Zheng, Z.B., Kerns, J., and Naganathan, S. (1995). Growth inhibition of hepatoma cells induced by vitamin K and its analogs. J. Biol. Chem. *270*, 28304–28310.
28. Groom, L.A., Sneddon, A.A., Alessi, D.R., Dowd, S., and Keyse, S.M. (1996). Differential regulation of the MAP, SAP and RK/p38 kinases by Pyst1, a novel cytosolic dual-specificity phosphatase. EMBO J. *15*, 3621–3632.
29. Dowd, S., Sneddon, A.A., and Keyse, S.M. (1998). Isolation of the human genes encoding the pyst1 and Pyst2 phosphatases: characterisation of Pyst2 as a cytosolic dual-specificity MAP kinase phosphatase and its catalytic activation by both MAP and SAP kinases. J. Cell Sci. *111*, 3389–3399.
30. Pu, L., Amoscato, A.A., Bier, M.E., and Lazo, J.S. (2002). Dual G1 and G2 phase inhibition by a novel, selective Cdc25 inhibitor 7-chloro-6-(2-morpholin-4-ylethylamino)-quinoline-5,8-dione. J. Biol. Chem. *277*, 46877–46885.
31. Rice, R.L., Rusnak, J.M., Yokokawa, F., Yokokawa, S., Messner, D.J., Boynton, A.L., Wipf, P., and Lazo, J.S. (1997). A targeted library of small-molecule, tyrosine, and dual-specificity phosphatase inhibitors derived from a rational core design and random side chain variation. Biochemistry *36*, 15965–15974.